Available online at www.sciencedirect.com

SCIENCE DIRECT®

Earth and Planetary Science Letters 229 (2005) 247–258

EPSL

www.elsevier.com/locate/epsl

Dynamics of continental rift propagation: the end-member modes

J.W. Van Wijk*, D.K. Blackman

IGPP, Scripps Institution of Oceanography UCSD, La Jolla CA 92093-0225, USA

Received 1 June 2004; received in revised form 8 October 2004; accepted 20 October 2004
Available online 15 December 2004
Editor: S. King

Abstract

An important aspect of continental rifting is the progressive variation of deformation style along the rift axis during rift propagation. In regions of rift propagation, specifically transition zones from continental rifting to seafloor spreading, it has been observed that contrasting styles of deformation along the axis of rift propagation are bounded by shear zones. The focus of this numerical modeling study is to look at dynamic processes near the tip of a weak zone in continental lithosphere. More specifically, this study explores how modeled rift behavior depends on the value of rheological parameters of the crust. A three-dimensional finite element model is used to simulate lithosphere deformation in an extensional regime. The chosen approach emphasizes understanding the tectonic forces involved in rift propagation. Dependent on plate strength, two end-member modes are distinguished. The stalled rift phase is characterized by absence of rift propagation for a certain amount of time. Extension beyond the edge of the rift tip is no longer localized but occurs over a very wide zone, which requires a buildup of shear stresses near the rift tip and significant intra-plate deformation. This stage represents a situation in which a rift meets a locked zone. Localized deformation changes to distributed deformation in the locked zone, and the two different deformation styles are balanced by a shear zone oriented perpendicular to the trend. In the alternative rift propagation mode, rift propagation is a continuous process when the initial crust is weak. The extension style does not change significantly along the rift axis and lengthening of the rift zone is not accompanied by a buildup of shear stresses. Model predictions address aspects of previously unexplained rift evolution in the Laptev Sea, and its contrast with the tectonic evolution of, for example, the Gulf of Aden and Woodlark Basin.

Keywords: lithosphere extension; rift propagation; transfer zone; finite element model; Laptev margin; Gulf of Aden

1. Introduction

An important aspect of continental rifting is that the deformation style varies progressively along the rift axis during rift propagation. Away from the pole of opening, lithosphere thinning increases and may eventually result in seafloor spreading. While continental deformation may be distributed, the rift to drift transition requires a focusing of deformation. In regions of rift propagation, specifically transition zones from continental rifting to seafloor spreading,

* Corresponding author. Fax: +1 858 534 5332.
E-mail address: jvanwijk@ucsd.edu (J.W. Van Wijk).

0012-821X/$ - see front matter © 2004 Elsevier B.V. All rights reserved.
doi:10.1016/j.epsl.2004.10.039

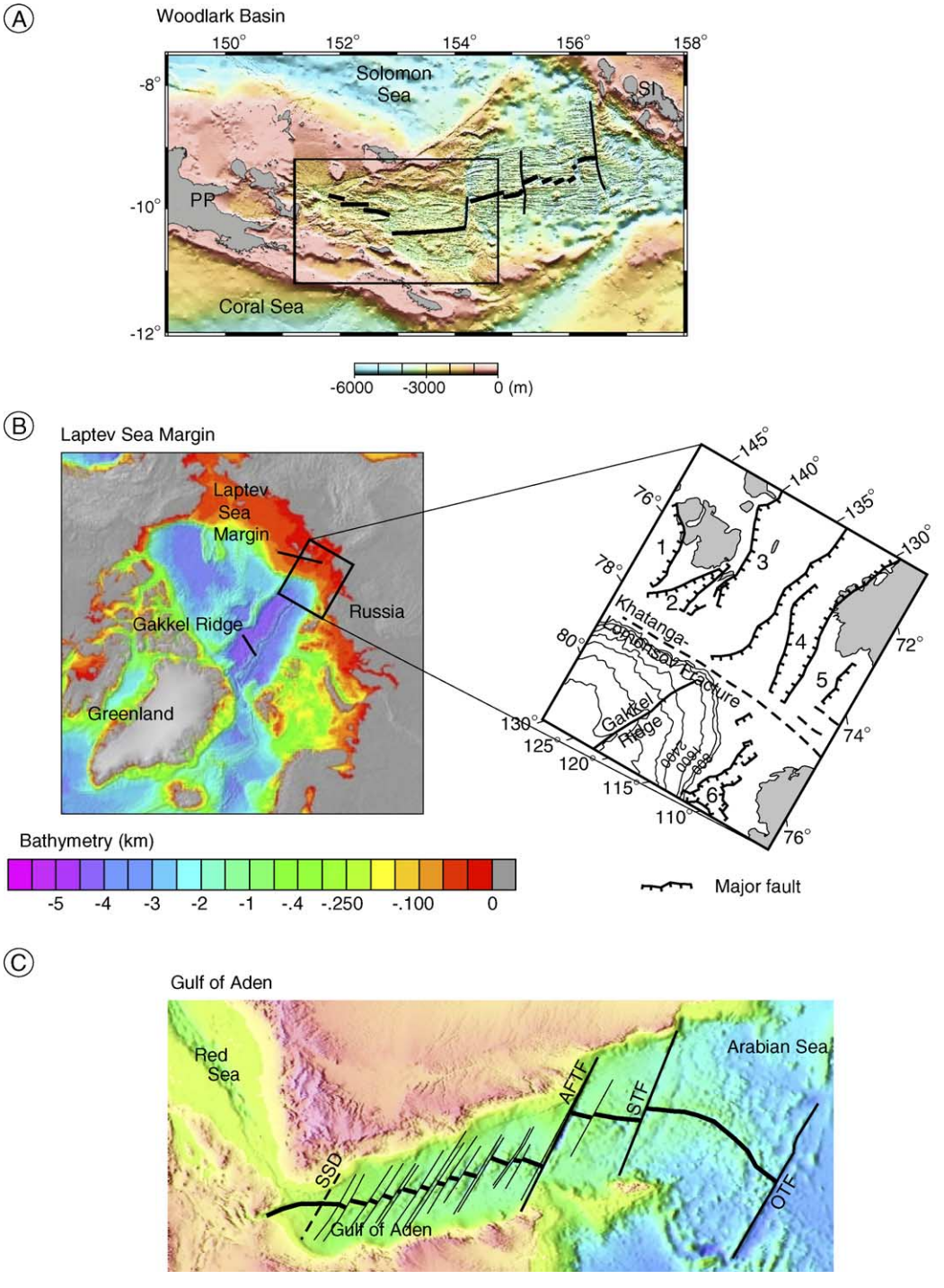
A
Woodlark Basin
150°
152°
154°
156°
158°
-8°
-10°
-12°
Solomon Sea
SI
PP
Coral Sea
-6000
-3000
0 (m)
B
Laptev Sea Margin
Laptev Sea Margin
Russia
Gakkel Ridge
Greenland
145°
140°
135°
130°
76°
78°
80°
72°
74°
1
2
3
4
5
6
Khatanga-Lomonosov Fracture
Gakkel Ridge
130°
125°
120°
115°
110°
Bathymetry (km)
-5
-4
-3
-2
-1
-.4
-.250
-.100
0
Major fault
C
Gulf of Aden
Red Sea
Arabian Sea
AFTF
STF
OTF
SSD
Gulf of Aden

contrasting styles of deformation along the axis of rift propagation are often bounded by shear zones. The transitional phase from continental rifting to active seafloor spreading can be found in a few places on earth. In the East Gakkel Ridge-Laptev Sea Margin area in the Arctic Ocean for example, an active spreading axis approaches a continental margin (Fig. 1). Here, the Gakkel spreading center terminates against a transform zone (the Khatanga-Lomonosov Fracture) that offsets the ridge from a wide zone of continental rifting (e.g., [1,3–5]). The currently most active continental rift segment on the Laptev Sea Margin is the Bel'Kov-Svyatoi Nos Rift, which is offset from the Gakkel Ridge over a distance of 150–200 km. This situation has persisted for over 50 million years (e.g., [1]), and magnetic lineation patterns indicate that the Gakkel Ridge is not propagating further at present; the rift to drift transition has stalled [6]. Different from the stalled rift situation of the Arctic in terms of a successful evolution of the rift to drift transition, is the Woodlark Basin off Papua New Guinea in the western Pacific. The Woodlark Basin-Papuan Peninsula region forms a continuous system of continental rifting and seafloor spreading (e.g., [7–12]; Fig. 1). Rapid continental extension initiated synchronously about 6 Ma [10] and was subsequently followed by the rift to drift transition. The different styles of rifting on the continental part of the rift and the oceanic spreading center are bounded by a currently developing transform fault system [7]. Formation of transform faults during pauses in the rift propagation process has also been observed in the Gulf of Aden [13,14]. The longest pause was at the Shukra-El Sheik discontinuity (SSD, Fig. 1), where rift propagation stalled for about 13 My [13], an earlier, shorter pause of 4 My occurred at the Alula-Fartak Fracture Zone. Shorter pauses and a slowing down propagation rate have been observed at other fracture zones in the Gulf of Aden. Manighetti et al. [13] found evidence for a relation between the occurrence of time breaks in propagation, formation of transform zones, and the encounter of the rift tip with different rheological provinces. It thus seems that continental rift propagation and rift to drift transition may evolve in an episodic manner, in which transform or shear zones are formed between the various extensional modes along the rift axis. It is a topic of debate whether large oceanic transform faults develop from such transfer or shear zones in continental rifts [9,15,16]. The time break between successive propagation periods varies considerably both within and between different extensional regions, ranging from less than 3 My (Gulf of Aden) to over 50 My (e.g., Gakkel Ridge).

It has generally been accepted that continental extension through heterogeneous lithosphere may ease or delay the rift propagation process. Rifting preferentially occurs along weak trends in the lithosphere, like thrust belts. In contrast, propagation of continental extension through a "locked" zone in the lithosphere may delay the rift to drift transition [17–19]. A locked zone could be formed, for example, by variations in rheological properties of the crust, an abnormally thickened crust or a less favorably oriented weak trend (i.e., a weak zone that is not parallel to the axis of maximum tensile stress), inherited from earlier tectonic events. Rift progression thus seems to be not only controlled by plate kinematics, but also by the inherited lithospheric structure.

The focus of this study is to look at dynamic processes near the tip of a weak trend in continental lithosphere. Our approach is probably best viewed as an attempt to understand the tectonic forces involved in rift propagation that may help to determine the interaction between continental and oceanic extensional regimes and processes responsible for the origin and evolution of continental breakup. A numerical model is used to study dynamic processes near a rift tip and possibilities for rift propagation. More specifically, this study explores how modeled rift behavior depends on the value of rheological parameters. Two end-member modes are distinguished. The stalled rift phase is characterized by absence of rift propagation for a certain amount of time. In the alternative rift

Fig. 1. (A) Multibeam bathymetry of Woodlark Basin [8]. Spreading ridge shown by thick black lines, major transform zones by thinner black lines. PP=Papuan Peninsula, SI=Solomon Islands. (B) Bathymetry and sketch of major fault structures of the Laptev Sea Margin. Dashed lines indicate strike-slip zones. Structural interpretation after [1]. 1. New Siberian Rift, 2. Anisin Rift, 3. Bel'Kov-Svyatoi Nos Rift, 4. Ust Lena Rift, 5. South Laptev Rift Basin, 6. West Laptev Rift Basin. (C) Topography and bathymetry of the Gulf of Aden and surrounding regions. Thick black line denotes the spreading ridge. SSD: Shukra El-Sheik discontinuity, AFTF: Alula Fartak transform fault, STF: Socotra transform fault, OTF: Owen transform fault. Segmentation pattern from [2,13].

Table 1
Thermal and rheological model parameters (same for all simulations)

Density [kg m^{-3}]	2700 (uc), 2800 (lc), 3300 (ml)
Thermal expansion [K^{-1}]	1×10^{-5}
Crustal heat production [W m^{-3}]	1×10^{-6}
Specific heat [J kg^{-1} K^{-1}]	1050
Conductivity [W m^{-1} K^{-1}]	2.6 (uc), 2.6 (lc), 3.1 (ml)
Young's modulus [Pa]	8×10^{10} (uc), 5×10^{10} (lc), 1×10^{10} (ml)
Poisson's ratio	0.25
Power-law breakdown stress [Pa]	600×10^{6}
Power-law exponent n	3.0 (olivine)
Activation energy Q [kJ mol^{-1}]	555 (olivine)
Material constant A [Pa^{-n} s^{-1}]	7.0×10^{-14} (olivine)

Parameters from [29,55,56]. uc is upper crust, lc is lower crust and ml is mantle lithosphere.

propagation mode, rift propagation occurs as a continuous process. Most rifting zones on earth probably evolve following a scenario in which the rift propagation process goes through different phases from continuous propagation interrupted by pauses when a locked zone is encountered, whereby the different deformation modes along the axis are balanced by shear zones or transform faults.

2. Models of discontinuous continental rifts

Prior three-dimensional numerical models on continental rifting approached different aspects of the process. They focused on pull-apart basins [20], or more in general on margin plateau formation [19]. The more local scale of this study precludes a two-dimensional elastic plate approach like that used in other rift propagation studies (e.g., [21]). Here, we use a thermo-mechanical approach to simulate extensional deformation of continental lithosphere. The mechanical part of the finite element code is based on Tecton [22–24]. It has been modified to be fully three-dimensional, allow for temperature-dependent power law rheology and buoyancy forces, and includes a correction for brittle/ductile behavior.

Visco-elastic deformation in the lithosphere is described in the numerical simulations by a Maxwell body:

$$\partial\varepsilon/\partial t = \sigma/2\mu \; + \; 1/E \; \partial\sigma/\partial t \qquad (1)$$

where ε is strain, μ is dynamic viscosity, σ is stress, t is time and E is Young's modulus. To represent the rheology of the lithosphere at low temperatures and stresses, where it approximates brittle deformation, it is assumed that rocks are fractured extensively, and strength is controlled by friction along preexisting faults, and Byerlee's law is adopted [25–28]. At high stresses, the value of the yield stress is given by the power law breakdown stress [29]. The state of stress is constrained by the force balance

$$\partial\sigma_{ij}/\partial x_j + \rho g_i = 0 \qquad (2)$$

in which g is gravity, ρ is density, and i,j vary 1–3 for x, y and z directions. In our simulations density follows a linear equation of state and only thermal buoyancy is considered:

$$\rho = \rho_0(1 - \alpha T). \qquad (3)$$

Here, α is the thermal expansion coefficient and T is temperature. Thermal expansion is believed to be the largest source of density gradients in the mantle beneath rifts. The mechanical part is coupled to a thermal finite element routine based on FELIB [30], where the heat flow equation is solved every time step on the same grid as the displacement field:

$$\rho c_p \mathrm{d}T/\mathrm{d}t = \partial_j k \partial_j T + H \qquad (4)$$

in which ρ is defined by Eq. (3), c_p is specific heat, k is conductivity and H is heat production in the crust, taken to be constant in the simulations. The parameter values used in the different tests are given in Tables 1 and 2. The Lagrangian formulation is used in the model, which means that crust and mantle material is attached to the nodal points. Mechanical and thermal parts are coupled through the temperature dependent power law rheology and equation of state, while advection of heat is accounted for by the nodal

Table 2
Crustal compositions used in the different simulations

	n	Q (kJ mol^{-1})	A (Pa^{-n} s^{-1})
Peridotite	3.3	532	3.9×10^{-16}
Quartz-diorite	2.4	219	5.0×10^{-18}
Granite	3.2	123	1.14×10^{-28}

Parameters from [55,56]. n is power-law exponent, Q is activation energy and A is material constant.

displacements. The relationship between stress and strain is described by

$$e = A\sigma^n \exp(-Q/RT) \quad (5)$$

where A is a material constant, n is the power law exponent, Q is activation energy and R is the gas constant. Eqs. (1)–(5) are solved using the finite element method, whereby the time step size is calculated according to the Courant criterion. The model domain is 1000×500×120 km ($x \times y \times z$). The mesh is non-equidistant, and grid spacing decreases gradually toward the zone of crustal weakness in the x-direction (5 km node spacing is used in the weak zone), toward the tip of this zone in the y-direction (node spacing is 3 km), and in the crustal layers (node spacing is 3 km). In the initial simulations presented below, numerical experiments are run for 4–7 My. With longer runs we find the grid to be seriously distorted, and this could affect the accuracy of the results. These initial numerical tests allow us to address overall behavior of the model, focusing on results that are robust despite the somewhat coarse node spacing. We defer discussion of other aspects of model predictions until additional, more computationally intensive experiments with finer node spacing can be completed.

Simulations are started with an equilibrium thermal state that is calculated using the boundary conditions and heat production in the crust. Because the crust is thickened in the weak zone (Fig. 2A), initial temperatures that are used to start the simulations are higher there (Fig. 2B). Displacements as a response to the applied initial and boundary conditions are calculated in the mechanical model. A constant temperature is adopted for the surface and base of the domain (respectively 0 and 1333 °C). Through the sides of the model a zero heat flow boundary condition is prescribed. Plate velocity boundary conditions for the mechanical model are applied in the negative and positive x-directions on the left and right sides (Fig. 2). The back and front sides are kept fixed in the y-direction (this is appropriate as long as the y boundaries are distant from regions of main interest such as a propagating tip, and along-strike flow is significantly less than across-strike flow) and free to move in x- and

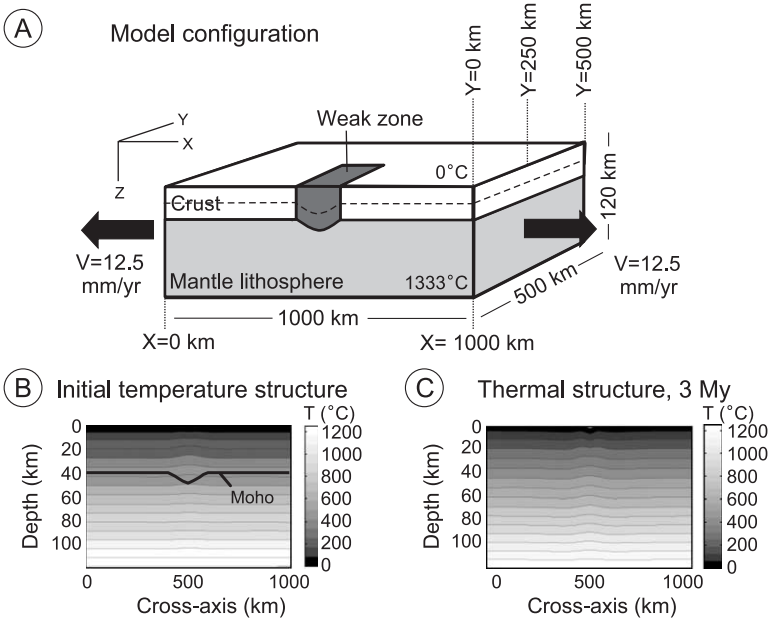

Fig. 2. (A) Model configuration. Lithosphere consists of crust and mantle portions. Dashed line is upper crust-lower crust boundary; upper crust and lower crust have same thickness. Crustal thickness is 40 km in the entire model domain except for the front part of the model domain ($y \leq 250$ km) where it is thickened in the center to 48 km to form a weak zone. Domain is extended with constant velocity of 25 mm/year (=total plate velocity). White layer is crust, dark gray denotes weak zone made of the same material as the rest of the crust, and light gray is mantle material. (B) Initial temperature field for a vertical transect through y=150 km for stalled rift case. (C) Thermal structure after 3 My of model evolution, vertical transect through y=150 km for stalled rift case.

z-directions. The base of the model is held horizontal but free to move in the x- and y-directions and the top surface is free to deform.

The lithosphere is rheologically layered and consists of crust and mantle lithosphere portions (Tables 1 and 2). The crust consists of an upper and lower crust of equal thickness (20 km each) and composition, but with different densities. Crustal rheologies vary between the different tests; for the mantle part of the domain an olivine composition is adopted. The choices of crustal rheologies are rather extreme; this enables studying end-member modes of the rift propagation process. It is assumed that the onset of intra-plate extension is the result of constructive interference of far-field forces and a tectonically thickened crust. The zone where crustal thickness is increased from its standard thickness of 40 km to a thickness of 48 km defines the weak zone (Fig. 2); the tectonically thickened crust is introduced in the model as an elongated area where the crust has been thickened by placing the Moho at a larger depth in the initial setup. In this way, stronger mantle material is replaced by weaker crust material. This, in combination with higher initial temperatures (Fig. 2B), creates a weak zone in the lithosphere. The width of the weak zone is 200 km from one side to the other, with significant crustal thickening (>4 km) in a 100 km wide zone. The weak zone is present between y=0 km and y=250 km (Fig. 2A), in the front portion of the model, and made of the same material as the rest of the crust. Upon extension of the lithosphere, deformation localizes in the weakened part of the lithosphere. Rifting there is recognized from crustal thinning and upwelling of the mantle in a subaxial zone, which causes elevated temperatures in this part of the lithosphere (Fig. 2C). Characteristics of the rift such as subsidence are not considered here as they could be more sensitive to processes not included such as sedimentation and erosion, and to the model resolution. Instead, the focus will be on the timing and location of rifting and dynamic processes near the rift tip, which are found to be robust predictions.

3. Results

3.1. Stalled rift

A very strong crustal rheology (peridotite, Table 2) results in a stalled rift situation. Predicted crustal thinning patterns are shown in Fig. 3A, crustal thinning

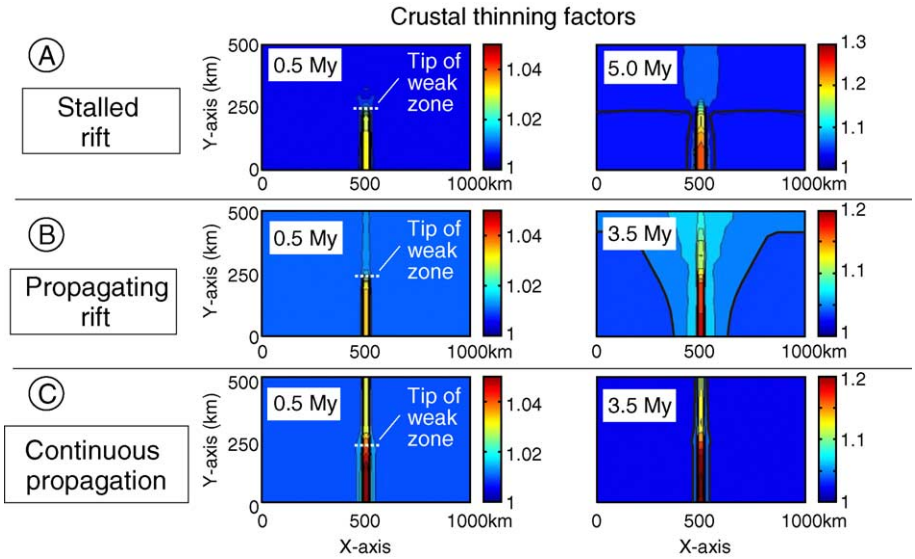

Fig. 3. Map view of crustal thinning factor. The crustal thinning factor is defined here as the ratio between the initial thickness of the crust and its current thickness. (A) Stalled rift mode. No rift propagation is predicted beyond the tip of the previously weakened zone. (B) Deformation is localized beyond the tip of the previously weakened zone, but propagation is not as fluently as in (C). (C) Continuous rift propagation mode. Left panels are from just after onset of extension (0.5 My), right panels after several My of extension. In left panels, initially prescribed end of the weak zone (at y=250 km) is indicated by white dashed line. Thick black lines in right panels denote thinning factor of 1.05.

factors are defined as the ratio between the initial crustal thickness and its present thickness. Deformation initiates simultaneously along the length of the weakened zone. Upon continuation of extension of the model domain, this rift does not propagate beyond the initially prescribed weakened zone; extensional stresses generated at the tip appear to be insufficient for rift propagation. The rift seems to "feel" the end of the weak zone and crustal thinning factors are strongly reduced toward the rift tip. As the model domain experiences ongoing extension and the back part of the model domain (where y>250 km) lacks any heterogeneities or weak zones, thinning of the crust in the back part is laterally almost uniform over the entire width of the domain to accommodate the stretching. Further evolution of the rift will occur within the rifted region but does not tend to step over the end of the weak zone.

Deformation is progressively less localized toward the region into which the rift is propagating and distributed over a wide zone crossing the tip of the weak trend. The rift-parallel (or y-) component of the velocity field (Fig. 4) shows that material flows toward the rift in the center of the domain. This process occurs both in the crust and mantle sections. In numerical modeling studies of oceanic ridge discontinuities the same pattern of the velocity field has been predicted near ridge ends in the upper mantle (e.g., [31]). An explanation for this flow is that it supplies some of the material that is dragged away from the rift axis by plate motion. The divergence of material is compensated by both upwelling and by north to south-directed rift-parallel flow. Also, upwelling is predicted to occur beyond the rift end in front of the propagator (in the back part of the domain). With one part of the plate rifted and the other part still almost undeformed, significant internal deformation of the plate is required. The simulations predict a concentration of horizontal shear stresses near the rift tip (Fig. 5A). The predicted shear zones are co-linear but have opposite sense of shear. They are located on the boundary between the two deformation styles, with an orientation that is, in this ideal situation, normal to the rift axis; they bound the wide and localized rift zones.

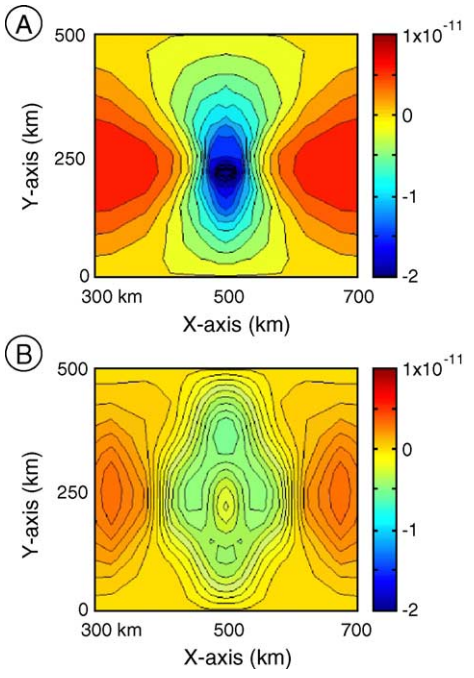

Fig. 4. (A) Rift-parallel (or y) component of velocity field in upper crust for stalled rift case and (B) continuous rift propagation case. Velocities in m/s, applied total extension rate is 25 mm/year. Map view at upper crustal depth of 9 km. Negative velocity values for north to south transport direction of material. Initial prescribed end of the weak trend is at y=250 km.

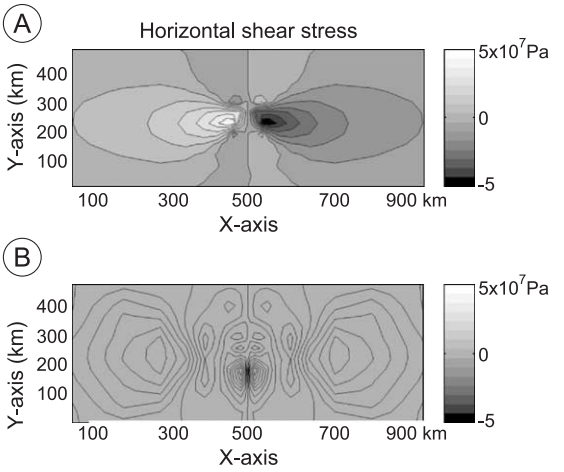

Fig. 5. Horizontal shear stresses for (A) stalled rift case and (B) continuous rift propagation case. Map view at upper crustal depth of 9 km. (A) Looking toward the backside of the domain, or toward increasing y-values, the right shear zone is left-lateral and the left shear zone is right-lateral.

3.2. Continuous rift propagation

Alternative to the stalled rift phase is the continuous rift propagation situation. When intermediate (quartz-

diorite) or weak (granite) crustal rheologies are chosen (Table 2), rifting is no longer limited to just a segment of the extended domain. In the case of a weak crustal rheology rifting initiates simultaneously in the entire weakened zone and beyond its end in the back part of the model domain, although there it is less prominent (Fig. 3C). The rift subsequently evolves and proceeds continuously in the direction of the back part of the domain. Rifting is localized along the entire rift axis and a clear rift tip as in the stalled rift case is not present. Extensional stresses at the tip of the propagator are sufficiently large for progressive evolution of the rift. The intermediate crustal strength results show similarities both with the continuous propagation results and with the stalled rift results. Rifting initiates simultaneously over the entire center of the domain but deformation is clearly less localized beyond the end of the weak zone (Fig. 3B). Proceeding of rifting is not as fast as in the weak crust case and deformation styles differ slightly along the rift axis, from localized rifting in the front part of the domain (y<250 km) to progressively more distributed extension as y increases.

When the structural styles of rifting between the two zones in the domain do become significantly different (as in the stalled rift case), this variation is predicted to be balanced out by a shear zone. Because of the absence of a variation in extensional modes for the propagating rift case, a buildup of shear stresses near the end of the weak zone is not expected (Fig. 5B), and not predicted by the numerical simulations. Also the rift-parallel component of the velocity field is different from the stalled rift case (Fig. 4B). The flow of material in the crust is not toward the negative y-direction, instead, a flow in the positive y-direction is predicted near the end of the initial weak zone. In time, this feature in the velocity field moves in the direction of rift propagation. This zone where rift-parallel flow is in the positive y-direction is rather localized, and velocities are directed toward the positive y-direction in a region about 50 km wide and 100 km long (Fig. 4B). Fig. 6 shows schematically the predicted difference between the velocity y-component of the stalled rift model and that of the continuous rift propagation model. In the stalled rift model, the flow direction of the rift parallel flow in the crust is directed in the negative y-direction near the rift tip or end of the weak zone (Fig. 6A), and this does not change during the evolution of the simulation (about 7 My for this

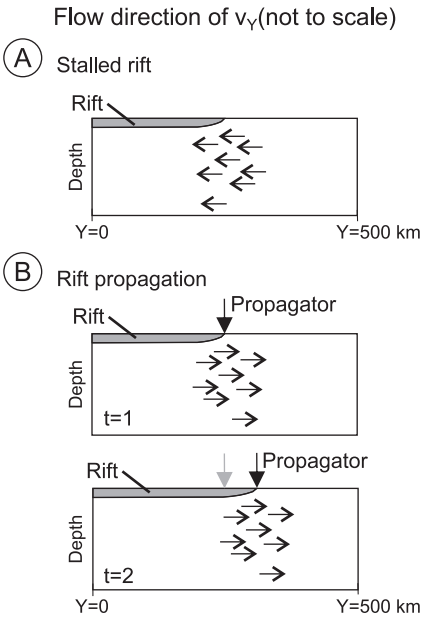

Fig. 6. Sketch of rift-parallel or y-component of velocity field in the crust. Shown are vertical transects through x=500 km, i.e. through the central axis of the rift for (A) the stalled rift case and (B) the continuous rift propagation case. (A) In the stalled rift case, the rift does not propagate into the positive y-direction. Material in the crust flows toward the rift tip (see also Fig. 4A and text for discussion). (B) In the rift propagation case, flow of crustal material is toward the positive y-direction, i.e. in the direction of rift propagation. The rift is shown schematically by the gray region. The propagator is placed where the crustal thinning factor is 1.05.

model). This flow supplies some of the material that is dragged away by the plate from the rift axis: material is not only supplied by upwelling, but by lateral flow as well. In the continuous rift propagation model, the flow is directed in the opposite direction, i.e. the positive y-direction, near the rift tip (Fig. 6B) in the crust. The location of this propagation-directed flow moves in time in the direction of rift propagation. When we (somewhat arbitrarily) take a crustal thinning factor of 1.05 to mark the tip of the propagating rift, calculated rift propagation velocities are about 10–17 cm/year during the continuous rift propagation phase.

Visco-elastic behavior of the lithosphere implies that progression of the rift tip can only occur when extensional stresses are generated more rapidly than they are relaxed by viscous relaxation. In the strong plate case high values of extensional stresses are needed in order for rifting to occur, while the weak or intermediate crustal strengths require lower extensional

stresses. According to the modeling results, extensional stresses built up near the rift tip are too low in the strong crust case, resulting in distributed deformation beyond the weak zone. This balance is different for weak and intermediate strength crustal compositions. It is likely that different thermal and boundary conditions and crustal structures may tip the scale to a different propagation mode.

4. Discussion and conclusion

When a propagating rift encounters a strong crust, inherited from prior geologic events, extensional stresses at the tip of the propagator may be insufficient for a continued propagation of the rift. Such rift blocking leads to formation of a transfer zone on the boundary between the two geologic provinces. An encounter with the locked zone may result in a pause in the rift propagation process during which extensional deformation within the locked zone may be very limited, distributed over a wide area, or offset from the original rift axis. The result is a discontinuity in the continental rifting as a consequence of inherited structures. With ongoing extension, two different adjacent spreading systems may develop, initiating at different times. Several studies have suggested [21,32] that large offsets in oceanic ridges could be relics of segmented continental spreading, although this link is difficult to establish in some areas [9,10]. On the tectono-magmatic segmented continental margin off Norway, Precambrian-age crustal sutures and weakness zones are linked to transfer zones on the margin and transform faults in the adjacent oceanic lithosphere [33,34]. For example, the Jan Mayen Lineament bounds high-density crustal bodies of probable Pre-Cambrian age, it separates the Møre and Vøring basins on the Norwegian margin, and is spatially connected to the Jan Mayen Fracture zone, a major transform fault system in the northern North Atlantic Ocean. Such margin segments, which are separated by transfer zones, typically differ from each other in terms of crustal structure, sediment distribution and vertical motions. Magnetic lineation patterns show that the oceanic ridge organizes itself after seafloor spreading commences into segments of variable length offset by discontinuities varying in nature and length. Mechanisms for continuing re-organization include passive or plate controlled segmentation and active or mantle upwelling controlled segmentation [35–38]. However, the initial fracture zone location could well be influenced by pre-breakup tectonic structures.

An example of a rift-propagation case in which the rift is stalled for a long time had previously appeared to not be supported by observations [10,17,39], but our predictions resemble some aspects of the East Gakkel Ridge- Laptev Sea shelf configuration and tectonic history. Recent geophysical and geological observations of the structure and dynamics of this ultra-slow spreading ridge and margin (e.g., [1,5,40–42]) rapidly improved knowledge of this area, and suggest that the Gakkel Ridge has basically stalled since about 50 My. Based on the wedge-shaped Laptev Sea margin bathymetry (Fig. 1) it has been suggested [1] that the Gakkel Ridge possibly propagated landward somewhat, but this has certainly been less successful than rift propagation in the Woodlark Basin, Gulf of Aden or the Red Sea [9,13,39]. Magnetic lineations show that seafloor spreading along the Gakkel Ridge started simultaneously at anomaly 24 (Paleocene, [3,43,44]). Prior to spreading, the area was affected by continental rifting since Late Cretaceous [45]. Formation of the continental basins on the Laptev shelf started probably in the Paleocene [4,5,45,46] and continues today [1,47,48]. The sheared continent-ocean transitional zone between the Gakkel Ridge and the Laptev Sea shelf is found to be narrow (<60 km) [1,48].

Analogues in the tectonic history and structural features between the stalled rift model predictions and Gakkel Ridge-Laptev Sea shelf include simultaneous localized deformation at the future plate boundary terminating at a shear zone that bounds a wide zone of continental rifting. Rocks with anomalous elastic properties have been sampled on the onshore part of the Laptev margin [1,4], but it is not known whether they indicate a very strong crustal rheology that, according to our modeling results, might inhibit rift propagation. Also, the thick sedimentary cover of the Laptev shelf [4,5] may have a thermal effect on the strength of the lithosphere. And, the spreading rate of the Gakkel Ridge decreases to ultra-slow (~8 mm/year) toward the Laptev margin. So, it is possible that the Laptev margin has consisted of a different tectonic province since continental extension took place in the Arctic region. However, because of lack of additional information on rheology, we can only speculate why

the rift stalled and why the present situation has existed for such a long time. Prior numerical modeling studies have shown that the duration of continental rifting until continental breakup occurs is dependent on factors such as the extension rate, Moho depth and topography, rheology and thermal structure [49–51], and that when the extension rate is sufficiently low with respect to lithospheric strength, continental breakup may not occur at all [52,53], instead, the locus of extension will migrate [53]. The fact that the continental rifting zone on the Laptev Margin is very wide, and the locus of extension has shifted in time [4], suggests that low extension rates with respect to the lithospheric strength in the region may have prohibited continental breakup. The stalled rift simulation shows that on the boundary between two such different tectonic settings a transfer zone is formed, which is in line with the large Khatanga-Lomonosov Fracture zone system, that balances contrasting focused deformation on the Gakkel Ridge plate boundary and distributed continental deformation on the Laptev Sea shelf.

The Arctic region differs from other rift to drift environments in the long duration of the stalled rift phase. Geological and geophysical observations of the Gulf of Aden [13] show time breaks varying between about 3 and 13 My, while even shorter episodes of non-propagation occurred in the Woodlark Basin. In the Gulf of Aden region these time breaks have been associated with the rift being less favorably oriented (i.e., the weak zone is not parallel to the axis of maximum tensile stress), or propagating into a structurally different tectonic province with a change in nature and rheology of the lithosphere. Between pauses in the propagating process, the spreading ridge in the Gulf of Aden propagated with an average velocity larger than 10 cm/year, and sometimes several tens of centimeter per year [13]. This observation is consistent with the large propagation rates predicted by our simulations. Oceanic spreading rates are larger in the Woodlark Basin and Gulf of Aden (~34 and ~15 mm/year, respectively) than in the Arctic Ocean (~8 mm/year). The larger extensional forces exerted on the rift may contribute to the shorter pauses in rift propagation in the Woodlark Basin, but also rheological and thermal properties of the lithosphere may contribute to the difference in stall duration.

Conceptual models of rift propagation and continental breakup, based on observations, generally agree on a succession of events in which a phase of geologically synchronous initiation of rifting along a segment of the rift axis is followed by a second phase of seafloor spreading [9,51,54]. Taylor et al. [10] propose that spreading center nucleation and possible ridge propagation form the second phase, in which the segmentation resulting from the continental-rifting phase is typically abandoned and new transform zones are formed. Other studies suggest that discontinuities in continental extension regions are related to discontinuities in oceanic ridges [14,38] that serve to accommodate along strike variations in extension and magmatism, although magmatic and geochemical segmentation in ocean spreading ridges do not always coincide well with pre-existing tectonic segmentation (e.g., [37,41]). Alternative models include punctiform asthenosphere upwelling propagating toward the pole of opening [32,51] following the first phase of continental rifting. In this study, rifting was not followed all the way to breakup and basically only the first phase of continental rifting has been simulated.

In summary, three-dimensional modeling of continental rifting in a coupled lithosphere/asthenosphere system predicts episodic propagation along the axis of opening. A stalled rift stage can occur when a rift meets a strong (locked) zone. Localized deformation changes to distributed deformation at the end of the rift, and the two different deformation styles are balanced by a shear zone oriented perpendicular to the rift axis. When a propagating rift meets a locked zone, whether in the form of different rheological parameters, variations in crustal thickness or other thermal, rheological or structural heterogeneities, it may cause a variation of deformation mode along its axis. The formation of a shear zone is required to balance the deformation on both sides. On the other side of the spectrum rift propagation can be a continuous process, when the crust outside the rift is of moderate or low strength relative to extension rates.

Acknowledgments

We thank two anonymous reviewers for their detailed and constructive comments that helped to improve this manuscript. This work was supported by grant OCE97-12164 and James G. Scripps Endowment match to EAR0105896.

References

[1] Ø. Engen, O. Eldholm, H. Bungum, The Arctic plate boundary, J. Geophys. Res. 108 (B2) (2003) 2075.

[2] P. Huchon, K. Khanbari, Rotation of the syn-rift stress field of the northern Gulf of Aden margin, Yemen, Tectonophysics 364 (2003) 147–166.

[3] Y. Kristoffersen, Eurasia Basin, in: A. Grantz, L. Johnson, J.F. Sweeney (Eds.), The Geology of North America, vol. L, Geological Society of America, Boulder, CO, 1990, pp. 365–378.

[4] S.S. Drachev, L.A. Savostin, V.G. Groshev, I.E. Bruni, Structure and geology of the continental shelf of the Laptev Sea Eastern Russia Arctic, Tectonophysics 298 (1998) 357–393.

[5] D. Franke, K. Hinz, O. Oncken, The Laptev Sea rift, Mar. Pet. Geol. 18 (2001) 1083–1127.

[6] H.A. Roeser, K. Hinz, A.L. Piskarev, S. Neben, Seafloor spreading at the transition from the Eurasia Basin to the Laptev shelf, Abstracts of the III International Conference on Arctic Margins, Germany, 1998, p. 155.

[7] V. Benes, S.D. Scott, R.A. Binns, Tectonics of rift propagation into a continental marginWestern Woodlark Basin, Papua New Guinea, J. Geophys. Res. 99 (1994) 4439–4455.

[8] A. Goodliffe, B. Taylor, F. Martinez, Data report: marine geophysical surveys of the Woodlark Basin region, in: B. Taylor, P. Huchon, A. Klaus, et al., (Eds.), Proc. ODP, Init. Repts., vol. 180, Ocean Drilling Program, College Station, TX, 1999, pp. 1–20.

[9] B. Taylor, A. Goodliffe, F. Martinez, R. Hey, Continental rifting and initial sea-floor spreading in the Woodlark basin, Nature 374 (1995) 534–537.

[10] B. Taylor, A.M. Goodliffe, F. Martinez, How continents break up: insights from Papua New Guinea, J. Geophys. Res. 104 (1999) 7497–7512.

[11] F. Martinez, A.M. Goodliffe, B. Taylor, Metamorphic core complex formation by density inversion and lower-crust extrusion, Nature 411 (2001) 930–934.

[12] G.A. Abers, A. Ferris, M. Craig, H. Davies, A.L. Lerner-Lam, J.C. Mutter, B. Taylor, Mantle compensation of active metamorphic core complexes at Woodlark rift in Papua New Guinea, Nature 418 (2002) 862–865.

[13] I. Manighetti, P. Tapponnier, V. Courtillot, S. Gruszow, P.-Y. Gillot, Propagation of rifting along the Arabia-Somalia plate boundary: the Gulfs of Aden and Tadjoura, J. Geophys. Res. 102 (1997) 2681–2710.

[14] E. D'Acremont, S. Leroy, M.O. Beslier, M. Fournier, N. Bellahsen, P. Patriat, M. Maia, P. Gente, From continental rifting to oceanic spreading: the conjugate passive margins of the eastern Gulf of Aden, Geophys. Res. Abstr. 6 (2004) 05802.

[15] K.D. Klitgord, J.C. Behrendt, Basin structure of the U.S. Atlantic margin, in: J.S. Watkins, L. Montadert, P.W. Dickerson (Eds.), Geological and Geophysical Investigations of Continental Margins, Memoir-American Association of Petroleum Geologists, vol. 29, 1979, pp. 85–112.

[16] G.S. Lister, M.A. Etheridge, P.A. Symonds, Detachment faulting and the evolution of passive continental margins, Geology 14 (1986) 246–250.

[17] V. Courtillot, Propagating rifts and continental breakup, Tectonics 1 (1982) 239–250.

[18] J.A. Dunbar, D.S. Sawyer, Patterns of continental extension along the conjugate margins of the central and north Atlantic Oceans and Labrador Sea, Tectonics 8 (1989) 1059–1077.

[19] J.A. Dunbar, D.S. Sawyer, Three-dimensional dynamic model of continental rift propagation and margin plateau formation, J. Geophys. Res. 101 (1996) 27845–27863.

[20] R. Katzman, U.S. ten Brink, J. Lin, Three-dimensional modeling of pull-apart basins: implications for the tectonics of the Dead Sea Basin, J. Geophys. Res. 100 (1995) 6295–6312.

[21] A. Hubert-Ferrari, G. King, I. Manighetti, R. Armijo, B. Meyer, P. Tapponnier, Long-term elasticity in the continental lithosphere; modeling the Aden Ridge propagation and the Anatolian extrusion process, Geophys. J. Int. 153 (2003) 111–132.

[22] H.J. Melosh, A. Raefsky, The dynamical origin of subduction zone topography, Geophys. J. R. Astron. Soc. 60 (1980) 333–354.

[23] H.J. Melosh, A. Raefsky, A simple and efficient method for introducing faults into finite element computations, Bull. Seismol. Soc. Am. 71 (1981) 1391–1400.

[24] H.J. Melosh, A. Raefsky, Anelastic response to dip slip earthquakes, J. Geophys. Res. 88 (1983) 515–526.

[25] J. Byerlee, Friction of rocks, Pure Appl. Geophys. 116 (1987) 615–626.

[26] C. Goetze, B. Evans, Stress and temperature in the bending lithosphere as constrained by experimental rock dynamics, Geophys. J. R. Astron. Soc. 59 (1979) 463–478.

[27] W.F. Brace, D.L. Kohlstedt, Limits on lithospheric stress imposed by laboratory experiments, J. Geophys. Res. 85 (1980) 6248–6252.

[28] R.C. Fletcher, B. Hallet, Unstable extension of the lithosphere: a mechanical model for Basin and Range structure, J. Geophys. Res. 88 (1983) 7457–7466.

[29] M.C. Tsenn, N.L. Carter, Upper limits of power law creep of rocks, Tectonophysics 136 (1987) 1–26.

[30] C. Greenough, K.R. Robinson, The finite element library. Release 4.0 (2000) (http://www.mathsoft.cse.clrc.ac.uk).

[31] Y. Shen, D.W. Forsyth, The effects of temperature- and pressure-dependent viscosity on three-dimensional passive flow of the mantle beneath a ridge-transform system, J. Geophys. Res. 97 (1992) 19717–19728.

[32] B.M. Abelson, A. Agnon, Mechanisms of oblique spreading and ridge segmentation, Earth Planet. Sci. Lett. 148 (1997) 405–421.

[33] F. Tsikalas, J.I. Faleide, O. Eldholm, Lateral variations in tectono-magmatic style along the Lofoten-Vesterålen volcanic margin off Norway, Mar. Pet. Geol. 18 (2001) 807–832.

[34] O. Eldolm, F. Tsikalas, J.I. Faleide, Continental margin off Norway 62–75°N: Paleogene tectono-magmatic segmentation and sedimentation, in: D.W. Jolley, B.R. Bell (Eds.), The North Atlantic igneous province: stratigraphy, tectonic, volcanic and magmatic processes, Geological Society, London, Special Publications, vol. 197, 2002, pp. 39–68.

[35] H. Schouten, K.D. Klitgord, J.A. Whitehead, Segmentation of mid-ocean ridges, Nature 317 (1985) 225–229.

[36] J. Phipps Morgan, E.M. Parmentier, Causes and rate-limiting mechanisms of ridge propagation: a fracture mechanics model, J. Geophys. Res. 90 (1985) 8603–8612.
[37] K.C. Macdonald, D.S. Scheirer, S.M. Carbotte, Mid-oceanic ridges: discontinuities, segments and giant cracks, Science 253 (1991) 986–994.
[38] N.R. Grindlay, P.J. Fox, K.C. Macdonald, Second-order ridge-axis discontinuities in the South Atlantic: morphology, structure and evolution, Mar. Geophys. Res. 13 (1991) 21–49.
[39] G.I. Omar, M.S. Steckler, Fission track evidence on the initial rifting of the Red Sea; two pulses, no propagation, Science 270 (1995) 1341–1344.
[40] H.J.B. Dick, J. Lin, H. Schouten, An ultraslow-spreading class of ocean ridge, Nature 426 (2003) 405–412.
[41] S.S. Drachev, N. Kaul, V.N. Beliaev, Eurasia spreading basin to Laptev Shelf transition: structural pattern and heat flow, Geophys. J. Int. 152 (2003) 688–698.
[42] P.J. Michael, C.H. Langmuir, H.J.B. Dick, J.E. Snow, S.L. Goldstein, D.W. Graham, K. Lehnert, G. Kurras, W. Jokat, R. Mühe, H.N. Edmonds, Magmatic and amagmatic seafloor generation at the ultraslow-spreading Gakkel ridge Arctic Ocean, Nature 423 (2003) 956–961.
[43] S.P. Srivastava, C.R. Tapscott, Plate kinematics of the North Atlantic, in: A. Grantz, L. Johnson, J.F. Sweeney (Eds.), The Geology of North America, vol. L, Geological Society of America, Boulder, CO, 1990, pp. 379–404.
[44] J.R. Cochran, G.J. Kurras, M.H. Edwards, B.J. Coakley, The Gakkel Ridge: Bathymetry, gravity anomalies, and crustal accretion at extremely slow spreading rates, J. Geophys. Res. 108 (B2) (2003) 2116.
[45] P.A. Ziegler, Evolution of the Arctic-North Atlantic and the western Tethys, Mem.-Am. Assoc. Pet. Geol. 43 (1988) 198.
[46] A.F. Grachev, Geodynamics of the transitional zone from the Moma Rift to the Gakkel Ridge, in: J.S. Watkins, C.L. Drake (Eds.), Studies in continental margin geology, Memoir-American Association of Petroleum Geologists, vol. 34, 1983, pp. 103–113.
[47] K. Fujita, D.B. Cook, The Arctic continental margin of eastern Siberia, in: A. Grantz, L. Johnson, J.F. Sweeney (Eds.), The Geology of North America, vol. L, Geological Society of America, Boulder, CO, 1990, pp. 289–304.
[48] D. Franke, F. Kruger, K. Klinge, Tectonics of the Laptev Sea-Moma Rift region: investigation with seismologic broadband data, J. Seismol. 4 (2000) 99–116.
[49] G. Bassi, Factors controlling the style of continental rifting: insights from numerical modeling, Earth Planet. Sci. Lett. 105 (1991) 430–452.
[50] J.W. van Wijk, R.S. Huismans, M. ter Voorde, S.A.P.L. Cloetingh, Melt generation at volcanic continental margins: no need for a mantle plume? Geophys. Res. Lett. 28 (2001) 3995–3998.
[51] G. Corti, J.W. van Wijk, M. Bonini, D. Sokoutis, S. Cloetingh, F. Innocenti, P. Manetti, Transition from continental break-up to punctiform seafloor spreading: how fast, symmetric and magmatic, Geophys. Res. Lett. 30 (12) (2003) 1604.
[52] P. England, Constraints on extension of continental lithosphere, J. Geophys. Res. 88 (1983) 1145–1152.
[53] J.W. van Wijk, S.A.P.L. Cloetingh, Basin migration caused by slow lithospheric extension, Earth Planet. Sci. Lett. 198 (2002) 275–288.
[54] E. Bonatti, Punctiform initiation of seafloor spreading in the Red Sea during transition from a continental to an oceanic rift, Nature 316 (1985) 33–37.
[55] G. Ranalli, Rheology of The Earth, 2nd ed., Chapman & Hall, 1995. 413 pp.
[56] S.H. Kirby, A.K. Kronenberg, Rheology of the lithosphere; selected topics, Rev. Geophys. 25 (1987) 1219–1244.